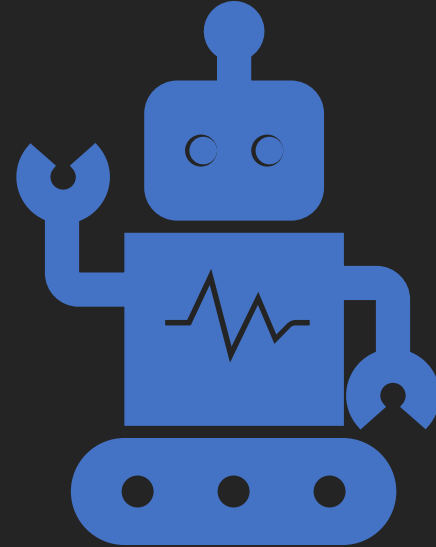


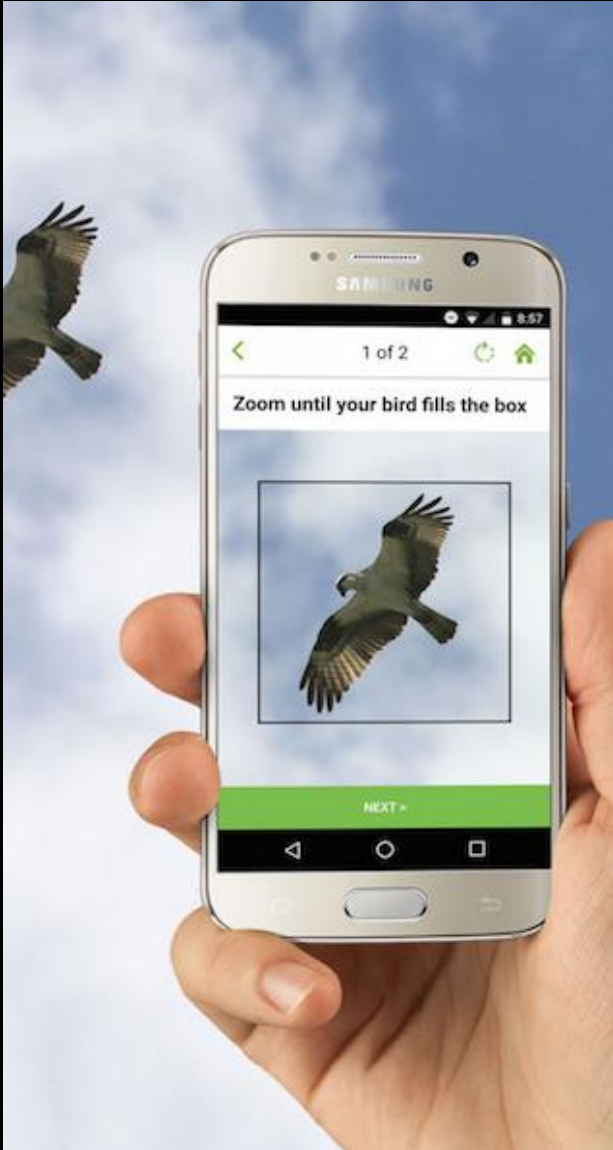
Apport de l'intelligence artificielle

Ingeborg Bajema



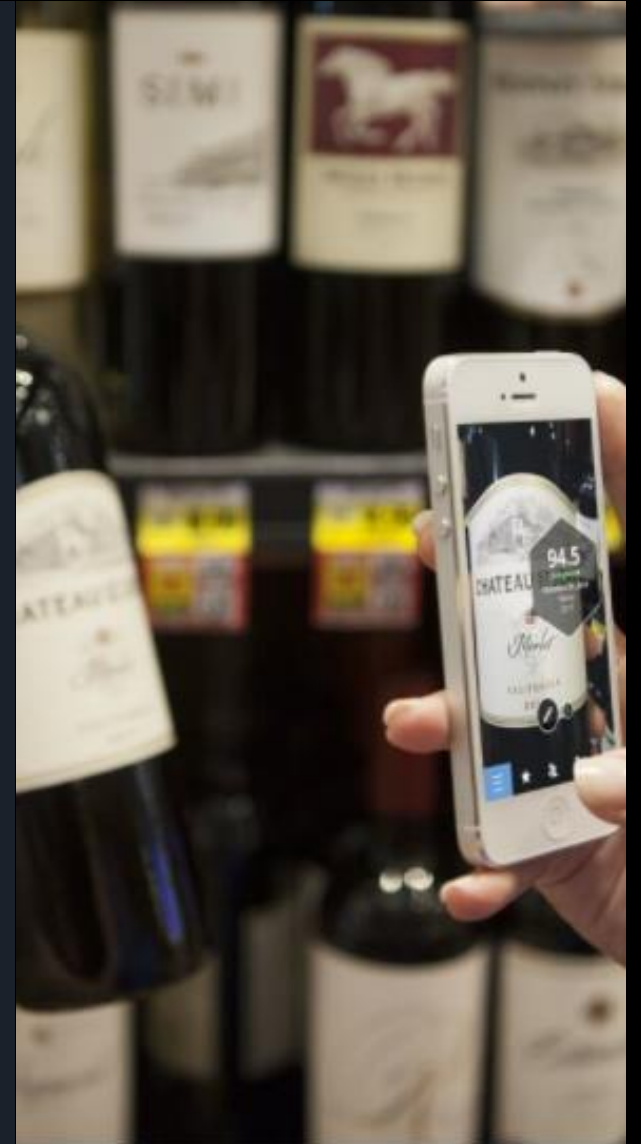
Disclosures

- **Consultancy:** GSK, Aurinia; Boehringer Ingelheim; Novartis; Toleranzia; CatBio
- **Other Interests or Relationships:**
 - Director of Bajema Institute of Pathology;
 - President of Renal Pathology Society;
 - Vice-President of European Vasculitis Society (EUVAS).

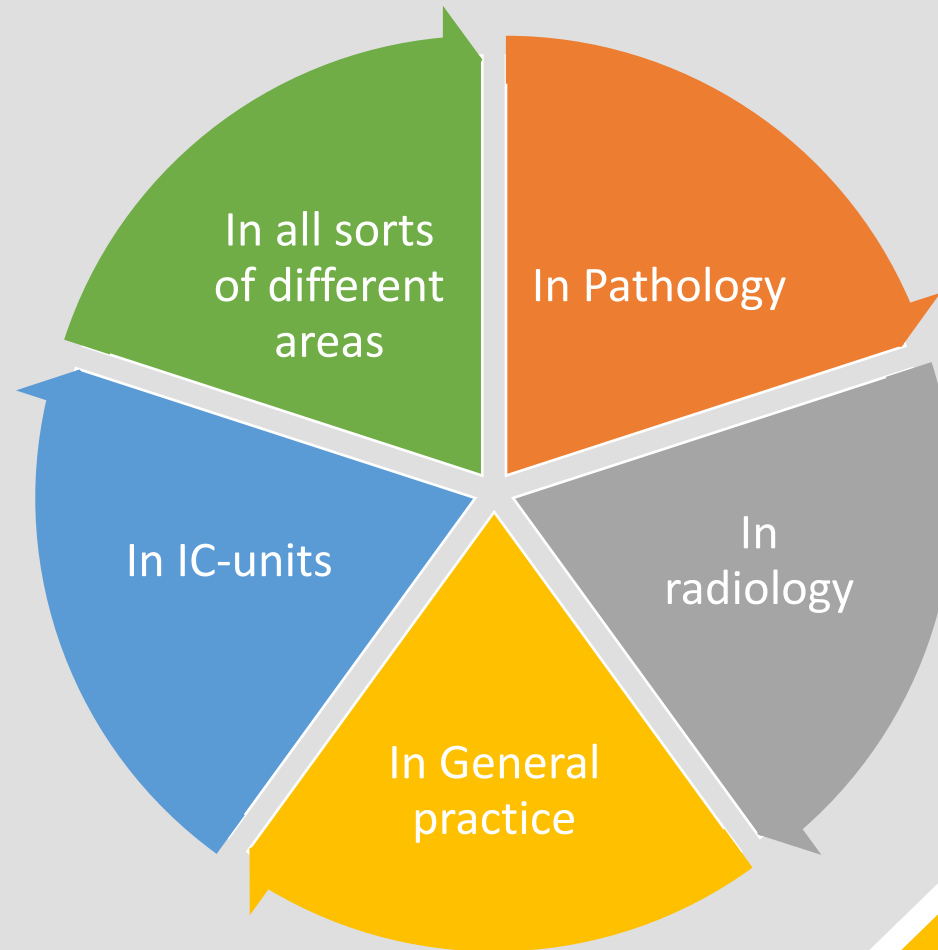


AI is everywhere!

- Think about:
- Bird-watching
 - Wine-appraisal
 - Google search on images



AI is
everywhere
in Medicine



Pubmed: last year over 30.000 publications on AI,
circa 10% on AI & pathology

30,589 results



Reset



Page

1

of 3,059



2021

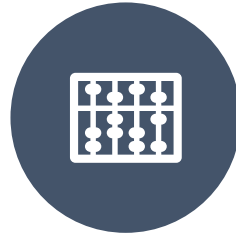
Nomenclature



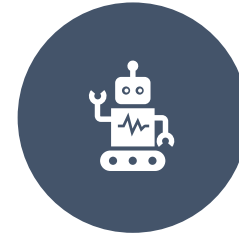
ARTIFICIAL
INTELLIGENCE (AI)



MACHINE LEARNING



DEEP LEARNING, BASED
ON CONVOLUTIONAL
NEURAL NETWORKS¹



ALGORITHMS





ETC

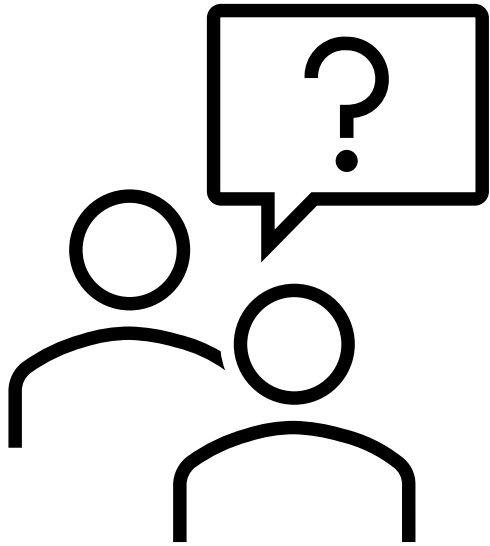
- Revolutionary speed in AI-assisted healthcare
- Synergetic developments of renal pathology and AI require **close interdisciplinary** collaborations between computer scientists and renal pathologists

REVIEW | [VOLUME 99, ISSUE 6, P1309-1320, JUNE 01, 2021](#)

AI applications in renal pathology

[Yuankai Huo](#) • [Ruining Deng](#) • [Quan Liu](#) • [Agnes B. Fogo](#) • [Haichun Yang](#)  

Published: February 10, 2021 • DOI: <https://doi.org/10.1016/j.kint.2021.01.015> •



IT language...

- U-net architecture
- To train the U-net architecture, 40 WSIs were divided into 5 subsets
- On each of the folds, a U-net was trained for 100 epochs
- There were 300 iterations per epoch with batch sizes of six patches
- Spatial and color augmentation techniques were applied to improve the algorithms robustness
- Adam was used as learning rate optimization algorithm
- Categorical cross entropy as loss function
- U-net models were applied as an ensemble for segmentation for all image sets
- The class with the highest probability was assigned as predicted label



Tissue slides



AI

Augmented Intelligence



Pathology report




A large orange circle on the left side of the slide, partially cut off by the edge.

Digitalized pathology

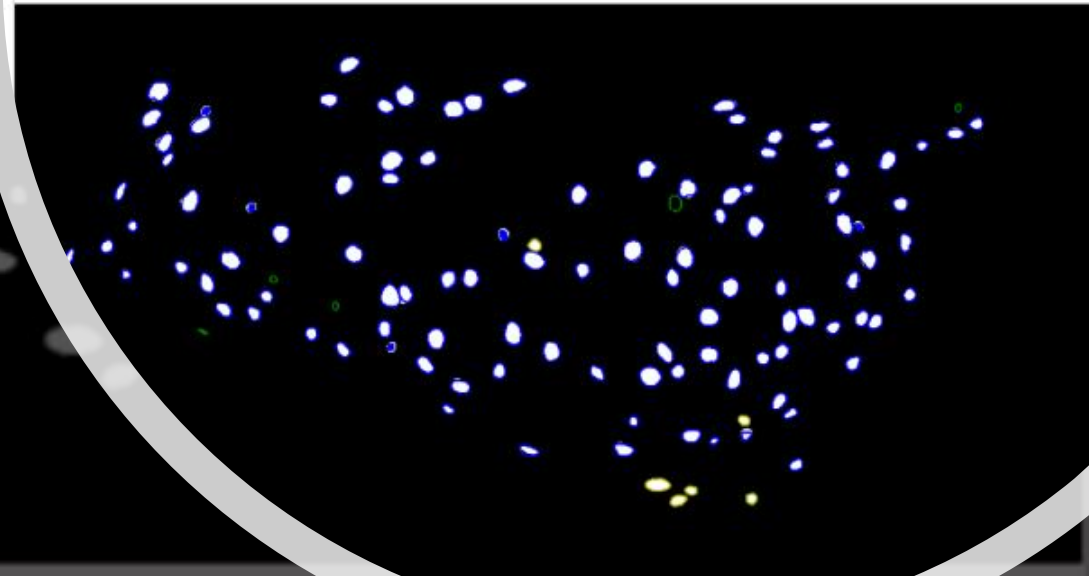
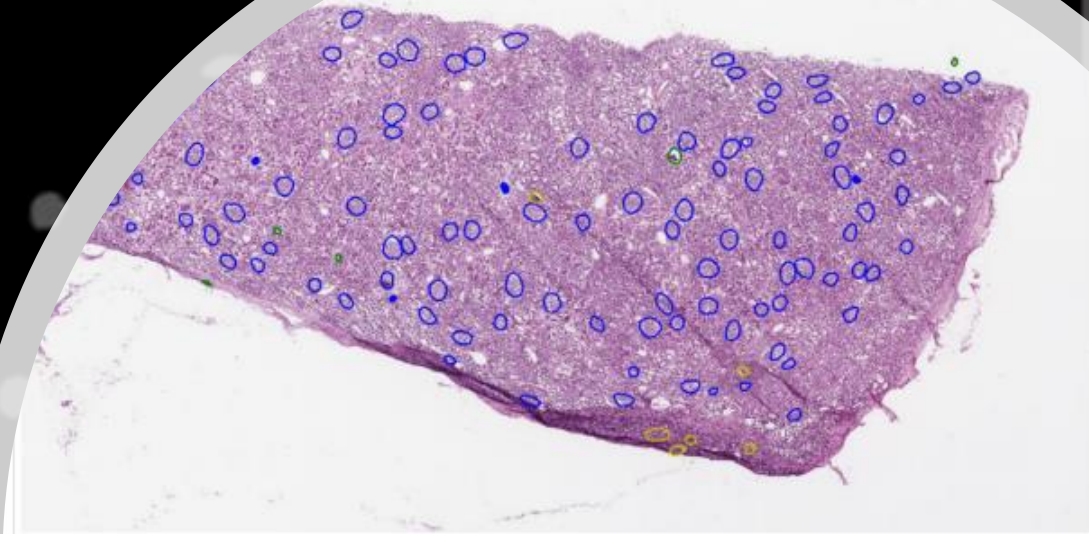
Scanned slides are the premise for
Artificial Intelligence in pathology

Benefits:

- 24/7 availability
 - Objective diagnostics
 - Relatively inexpensive
 - Interobserver variability reduction
- 
- A yellow dashed line in the bottom right corner, consisting of several short, curved segments.

Annotation of anatomical
structure on a digitalized
whole slide image (WSI)

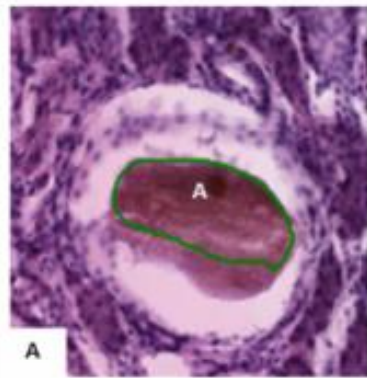
The algorithm learns how to
recognize the structure



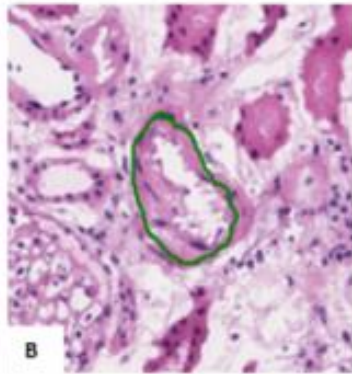
Development and evaluation of deep learning–based segmentation of histologic structures in the kidney cortex with multiple histologic stains.

Sclerotic Model

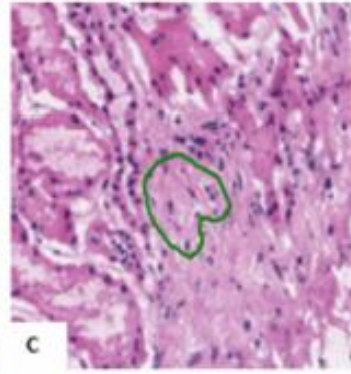
False Positive



Intratubular cast –
processing artifacts

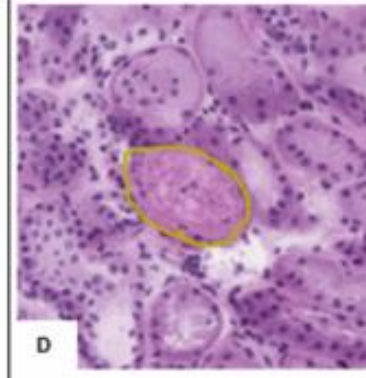


Small artery – mild
intima fibrosis

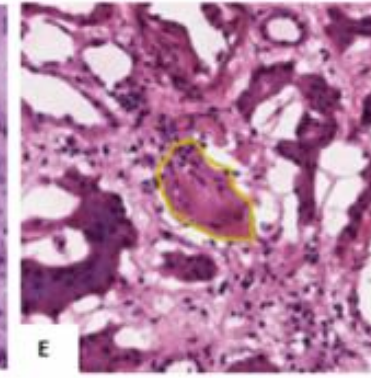


Interstitium – matrix with
sparse nuclei

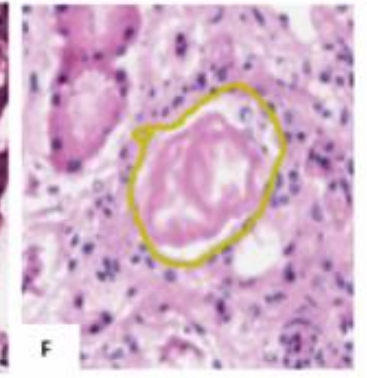
False Negative



Global sclerosis –
Textural heterogeneity



Global sclerosis -
Processing artifacts



Global sclerosis –
Textural heterogeneity



kidney
INTERNATIONAL

OFFICIAL JOURNAL OF THE INTERNATIONAL SOCIETY OF NEPHROLOGY

Jayapandian, Chen et al, 2020

Development and evaluation of deep learning–based segmentation of histologic structures in the kidney cortex with multiple histologic stains.

Study Aims:

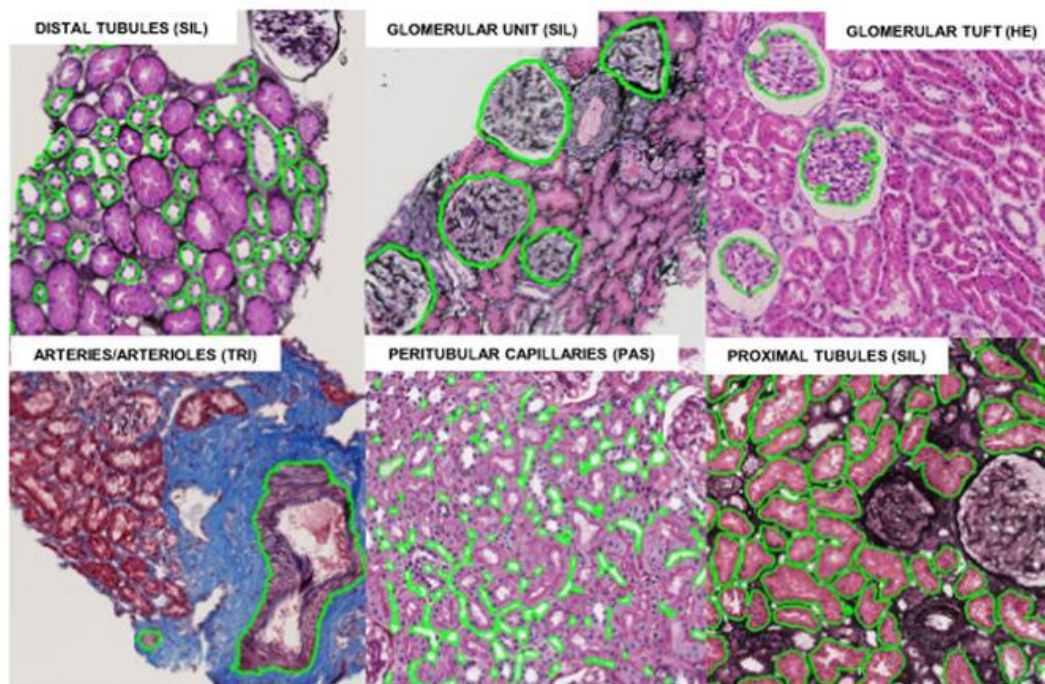
Novel protocols for renal biopsy assessment

Feasibility of deep learning-based (DL) convolutional neural networks (CNNs) for normal histology, to facilitate quantitation of prognostic histologic structures

Dataset:

- 125 NEPTUNE MCD **biopsies**
- H&E, PAS, TRI, SIL **stains**
- 459 WSIs of **normal renal** parenchyma (MCD)
- 38 **pathology** laboratories
- 30048 **annotations** generated across primitives

U-Net DL Segmentation using multistained WSIs

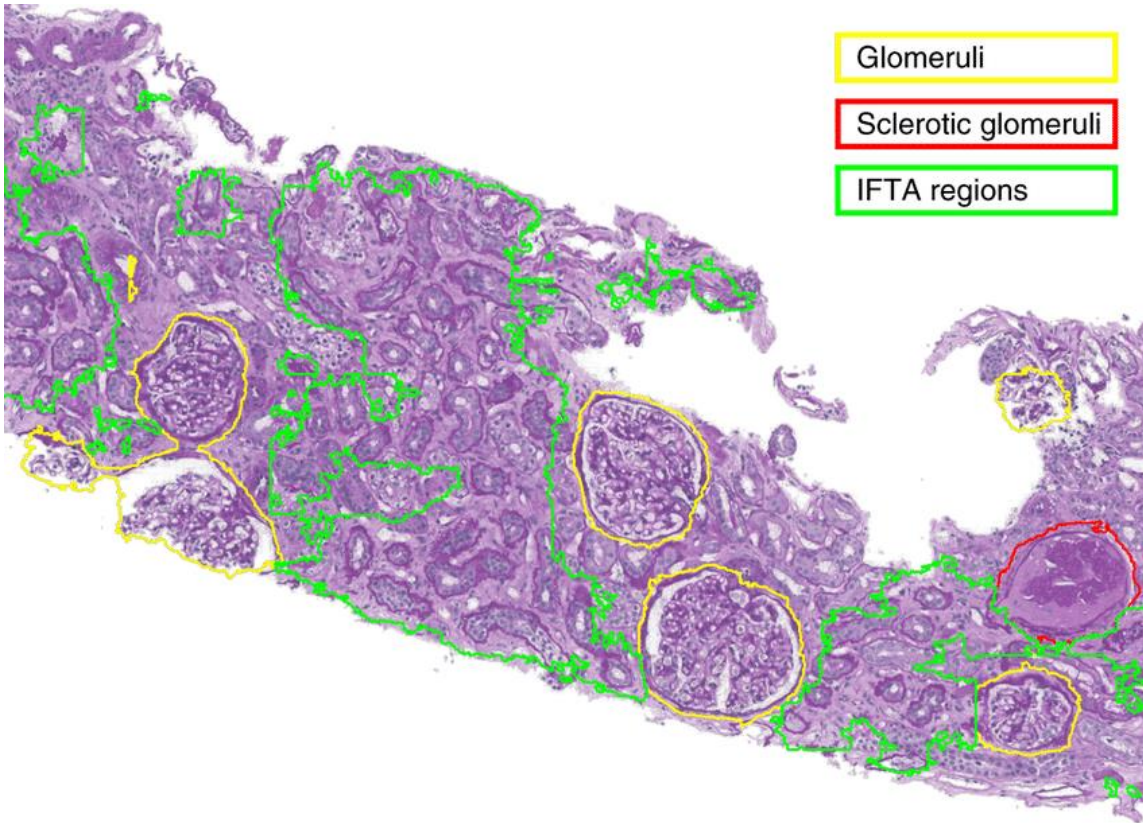


Results:

- Comparative DL **performance** across 4 stains (Best results on PAS stained WSIs)
- **Multiple** DL networks with suggested number of training exemplars across primitives
- **Optimal** digital magnification: 5X glomeruli, 10X tubules and arteries, 40X peritubular capillaries
- Validated on **nephrectomies**
- **Online** access to data and tutorials to setup DL networks

CONCLUSION:

DL-based CNNs permit **efficient** segmentation of kidney histologic structures on **multiple stains** with substantial **tissue heterogeneity** across centers. This work creates a technical foundation to support **pathology workflows** for better **disease characterization** and **risk assessment**.



Articles

<https://doi.org/10.1038/s42256-019-0018-3>

nature
machine intelligence

An integrated iterative annotation technique for easing neural network training in medical image analysis

Brendon Lutnick¹, Brandon Ginley¹, Darshana Govind¹, Sean D. McGarry², Peter S. LaViolette³, Rabi Yacoub⁴, Sanjay Jain⁵, John E. Tomaszewski¹, Kuang-Yu Jen⁶ and Pinaki Sarder^{1*}

HITL: Human in the loop for segmentation refinement

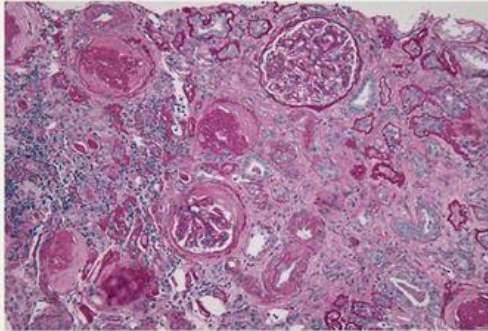
Prognostic Value of Histopathologic Lesions in Native Kidney Biopsy Specimens

METHODS

Prospective cohort study

3 tertiary care hospitals

676 individuals undergoing native kidney biopsy

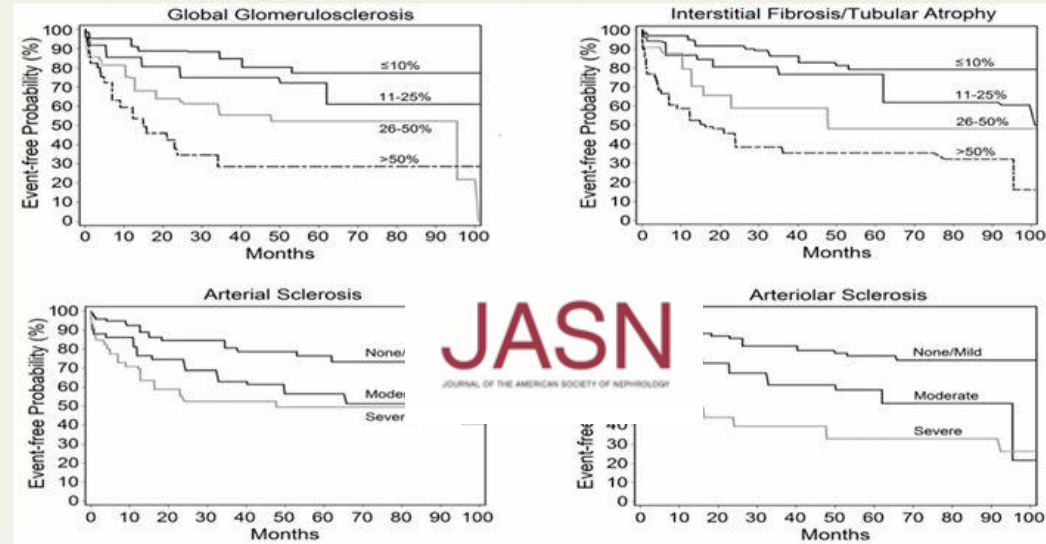


13 histopathological lesions graded semi-quantitatively

Histopathological lesions were tested for association with kidney disease progression over median follow-up time of 34.3 months

OUTCOME

Risk of 40% decline in eGFR or renal replacement therapy



Generalized log-rank $P < 0.001$

CONCLUSION Semi-quantitative scores of histopathologic lesions provide prognostic information independent of eGFR, proteinuria, and other clinical variables.

Across a diverse group of kidney diseases, histopathologic lesions on kidney biopsy provide prognostic information, even after adjustment for proteinuria and eGFR.

JASN

Anand Srivastava,^{1,2} Ragnar Palsson,¹ Arnaud D. Kaze,¹ Margaret E. Chen,¹ Polly Palacios,¹ Venkata Sabbiseti,¹ Rebecca A. Betensky,³ Theodore I. Steinman,⁴ Ravi I. Thadhani,^{5,6,7} Gearoid M. McMahon,¹ Isaac E. Stillman,⁸ Helmut G. Rennke,⁹ and Sushrut S. Waikar¹

Deep learning-based histopathological assessment of renal tissue

TRAINING

- 40 transplant biopsies
- 10 tissue classes
- 9488 annotations

TEST

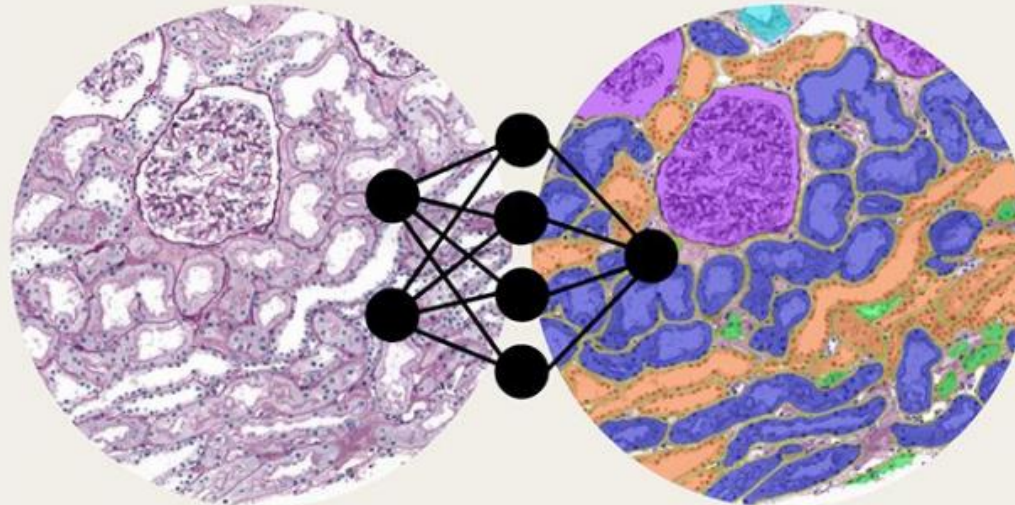
- 20 transplant biopsies from two centers
- 15 nephrectomy samples
- 82 transplant biopsies for correlation with visual (Banff) scoring of multiple pathologists

LEGEND

- Border
- Glomeruli
- Undefined tubuli
- Proximal tubuli
- Distal tubuli
- Atrophic tubuli
- Arteries

No fill = interstitium

Convolutional Neural Network for segmentation renal tissue



RESULTS

- Highest performance for glomeruli, tubuli and interstitium segmentation
- Average DC¹ 0.88
- Equal performance on images **external center**
- For analysis of **nephrectomy and biopsy** samples
- For **healthy** and **pathological** tissue
- CNN-based quantifications **correlate significantly** with components **Banff** scoring system

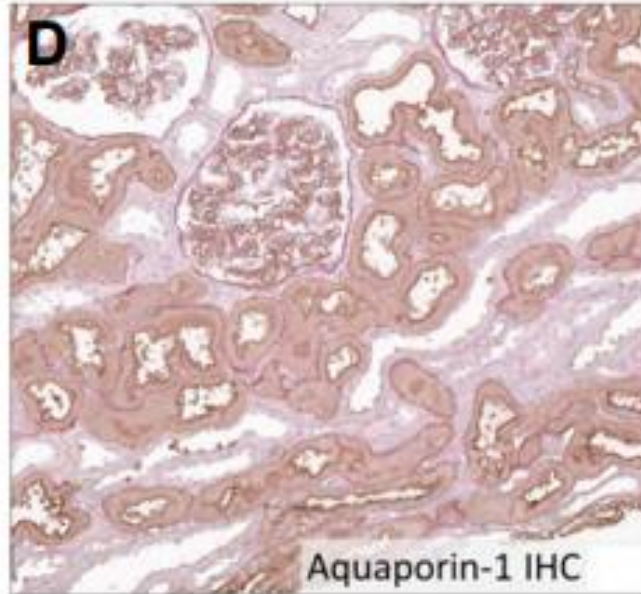
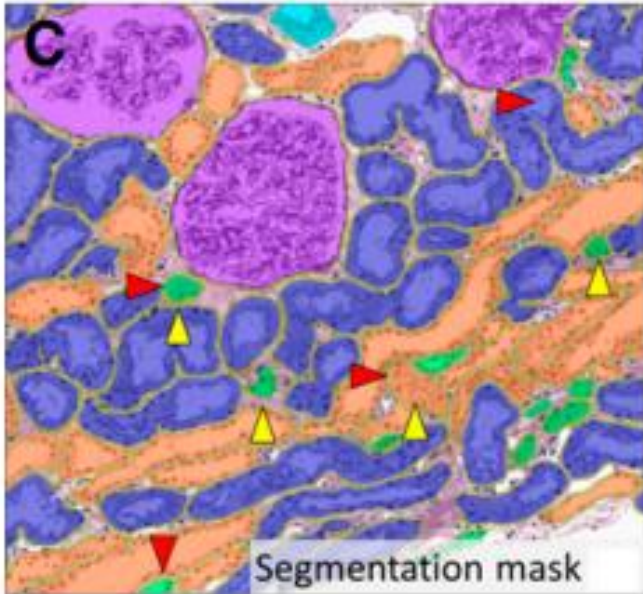
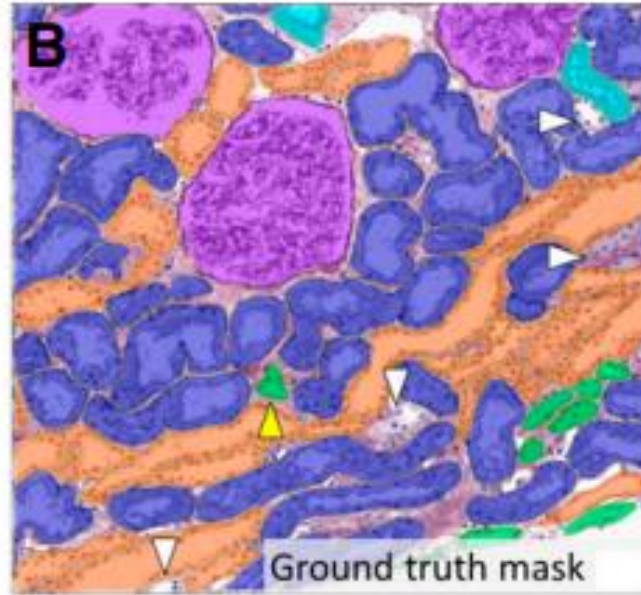
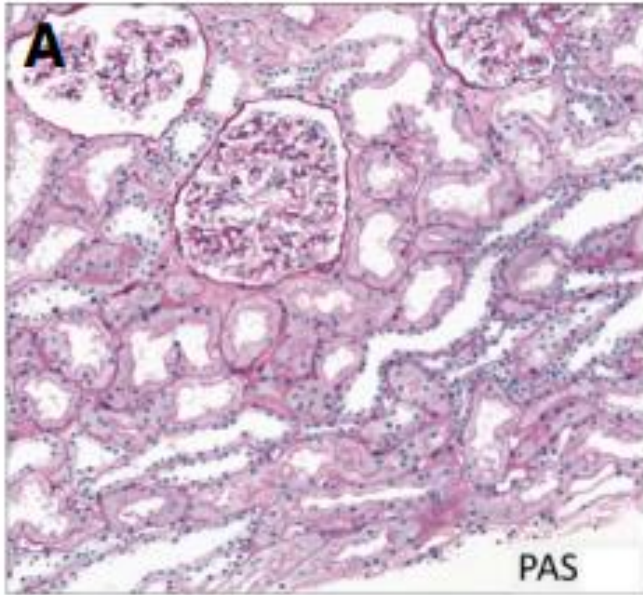
CONCLUSION

This study presents **the first CNN for multi-class segmentation** of periodic acid-Schiff-stained **nephrectomy samples and transplant biopsies**. Our CNN can be of aid for quantitative studies concerning renal histopathology **across centers** and provides opportunities for deep learning applications in routine diagnostics.

¹DC= Dice coefficient

Jesper Kers*, Roman D Bülow*, Barbara M Klinkhammer, Gerben E Breimer, Francesco Fontana, Adeyemi Adefidipe Abiola, Rianne Hofstra, Garry L Corthals, Hessel Peters-Sengers, Sonja Djudjaj, Saskia von Stillfried, David L Holscher, Tobias T Pieters, Arjan D van Zuilen, Frederike J Bemelman, Azam S Nurmohamed, Maarten Naesens, Joris J T H Roelofs, Sandrine Florquin, Jürgen Floege, Tri Q Nguyen, Jakob N Kather†, Peter Boor†

JASN
JOURNAL OF THE AMERICAN SOCIETY OF NEPHROLOGY



A: represents regions used for testing
 B: manually produced ground truth
 C: The CNN's result
 D: IH to highlight proximal tubules
 Yellow arrowhead: inconsistency with IH
 White arrowhead: annotation error
 There is a large overlap between B and C

- Border
- Interstitium
- Glomeruli
- Sclerotic glomeruli
- Empty Bowman's capsule
- Proximal tubuli
- Distal tubuli
- Atrophic tubuli
- Undefined tubuli
- Capsule
- Arteries

CNN versus BANFF Classification System

The network's applicability for *routine diagnostic tasks* was assessed by comparing the CNN's quantification of a selection of structures to visually scored histologic (Banff) components in 82 PAS-stained transplant biopsies.

The ICCs for glomerular counting by the CNN and the pathologists ranged from 0.93 to 0.96

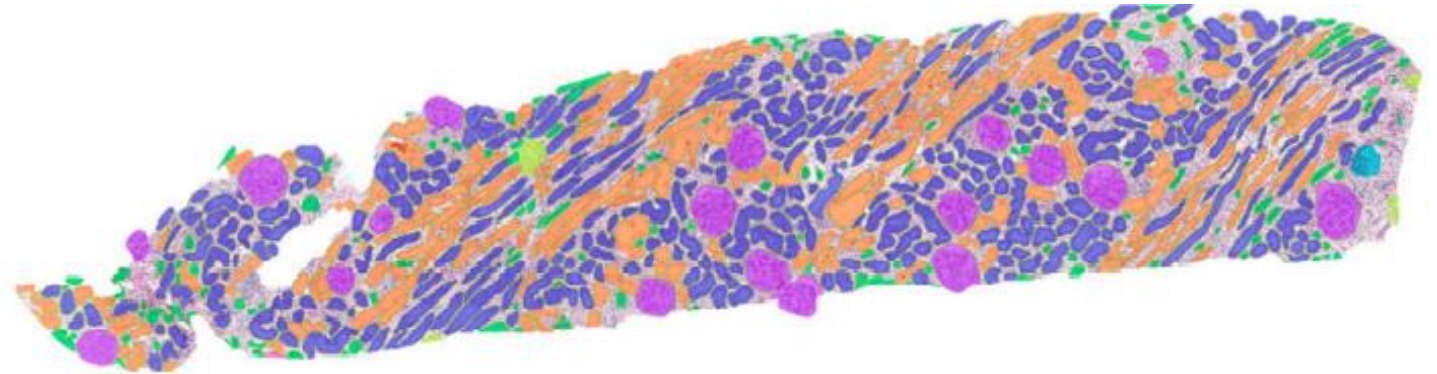



TABLE 2.**This is a synopsis of the thresholds for all Banff Lesion Scores**

Banff lesion score,	Abbreviation	0	1	2	3
Interstitial inflammation	<i>i</i>	<10%	10-25%	26-50%	>50
Tubulitis	<i>t</i>	None	1-4/tubular cross section or 10 tubular epithelial cells	5-10	>10 or foci of tubular basement membrane destruction with $i \geq 2$ and $t2$ elsewhere
Intimal arteritis	<i>v</i>	None	<25% luminal area lost	$\geq 25\%$ luminal area lost	Transmural and/or fibrinoid change and medial smooth muscle necrosis
Glomerulitis	<i>g</i>	None	<25%	25-75%	>75%
Peritubular capillaritis	<i>ptc</i>	<3 leukocytes/ PTC	≥ 1 leukocyte in $\geq 10\%$ of PTCs with max. of 3-4/PTC	≥ 1 leukocyte in $\geq 10\%$ of PTCs with max. of 5-10/PTC	≥ 1 leukocyte in $\geq 10\%$ of PTCs with max. of >10/PTC
C4d	<i>C4d</i>	None	<10%	10-50%	>50%
Interstitial fibrosis	<i>ci</i>	$\leq 5\%$	6-25%	26-50%	>50%
Tubular atrophy	<i>ct</i>	None	$\leq 25\%$	26-50%	>50%
Vascular fibrous Intimal thickening	<i>cv</i>	None	$\leq 25\%$	26-50%	>50%
GBM double contours	<i>cg</i>	None	1a: only by EM 1b: $\leq 25\%$ by LM	26-50%	>50%
Mesangial matrix expansion	<i>mm</i>	None	$\leq 25\%$	26-50%	>50%
Arteriolar hyalinosis	<i>ah</i>	None	Mild to moderate in ≥ 1	Moderate to severe in >1	Severe in many
Hyaline arteriolar thickening	<i>aah</i>	None	1 without circumferential	≥ 1 without circumferential	circumferential

Artificial intelligence applications for pre-implantation kidney biopsy pathology practice: a systematic review

Ilaria Girolami¹ · Liron Pantanowitz² · Stefano Marletta³ · Meyke Hermesen⁴ · Jeroen van der Laak⁴ · Enrico Munari⁵ · Lucrezia Furian⁶ · Fabio Vistoli⁷ · Gianluigi Zaza⁸ · Massimo Cardillo⁹ · Loreto Gesualdo¹⁰ · Giovanni Gambaro¹¹ · Albino Eccher¹² 

CNN architecture for semantic segmentation with two models	Global accuracy higher than 0.98; precision in classifying healthy and sclerosed glomeruli ranging 0.834–0.935 and 0.806–0.976
Two-layer, error back-propagation ANN	Accuracy higher than 0.93, precision higher than 0.88 in validation set and higher than 0.91 in test set
Shallow ANN	0.99 accuracy, 1.00 precision
Patch-based and fully CNN model	Fully CNN model with greater correlation with percent global glomerulosclerosis ($R^2=0.828$); robust to preparation artifacts
Deep-learning model based on the model of previous study	Higher correlation of model with ground truth annotations ($r=0.916$) than on-call pathologists; lower quota of kidneys classified as to be discarded respect to on-call pathologists
RENFAST model: semantic segmentation CNN model	Accuracy 0.89–0.94 for vessel detection with Dice score 0.83–0.84; accuracy 0.92 for interstitial fibrosis; 2 min of computation time against 20 min for pathologists
RENTAG model: semantic segmentation CNN model	Dice score of 0.95 and 0.91 for glomeruli and tubuli detection; 100% sensitivity and PPV; little time of computation required

Deep Learning based segmentation and quantification in experimental kidney histopathology

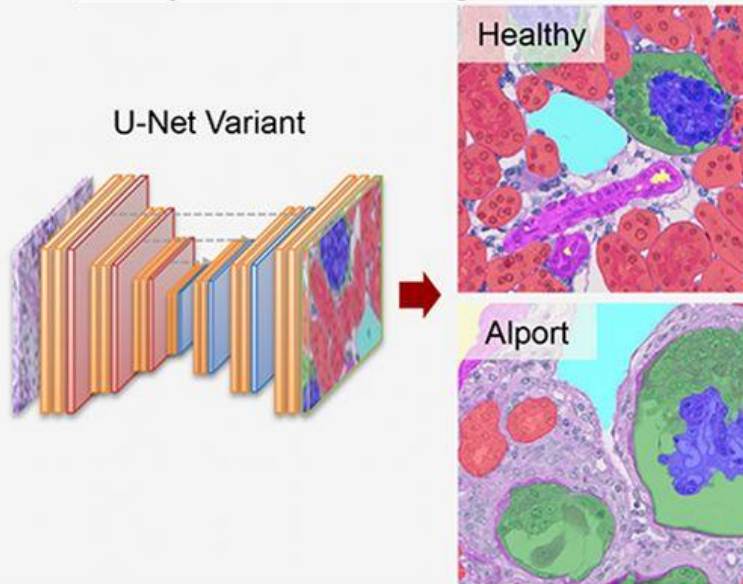
JASN

JOURNAL OF THE AMERICAN SOCIETY OF NEPHROLOGY

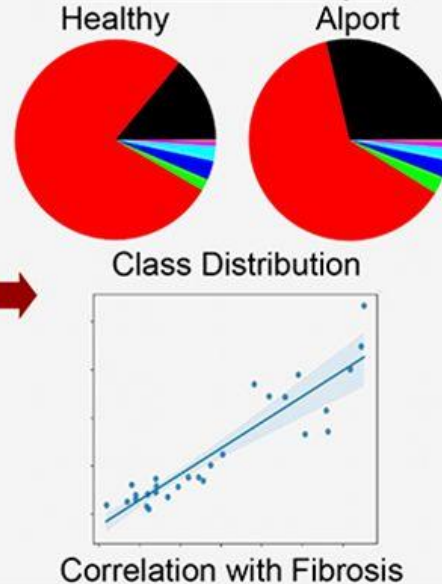
METHODS

- 5 murine disease models, 6 species (Mouse, Rat, Pig, Marmoset, Bear, Human)
- 72722 Annotations in 2930 patches (2100 Train. / 160 Val. / 670 Test)
- Classes: • **Tubule** • **Glomerular tuft** • **Full glomerulus** • **Artery**
• **Arterial lumen** • **Vein** • Remaining tissue

Kidney Whole Slide Segmentation



Quantitative Analysis

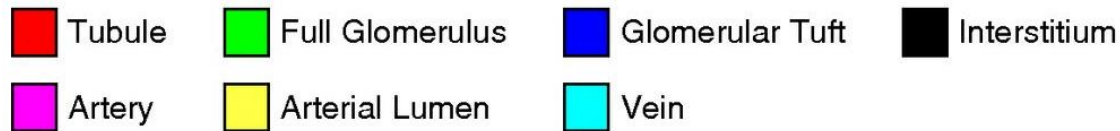
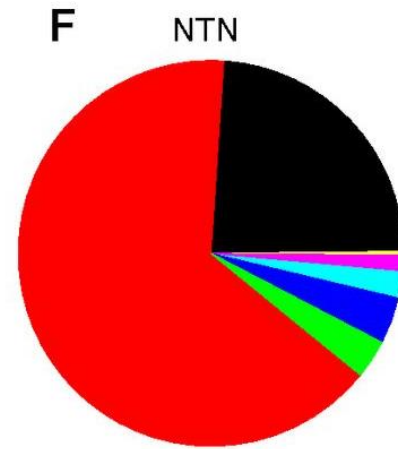
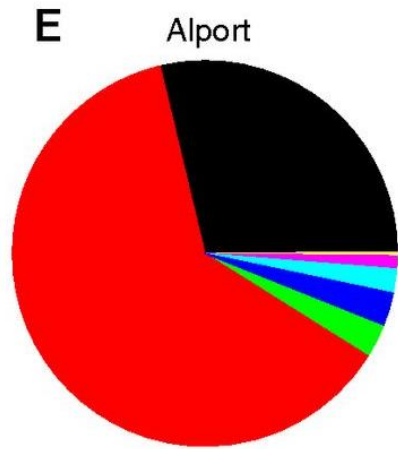
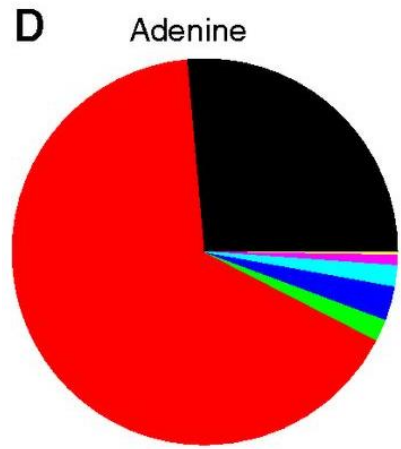
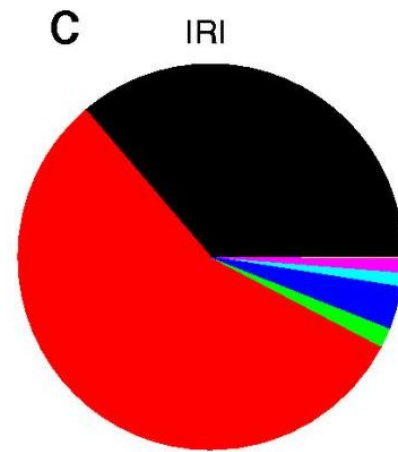
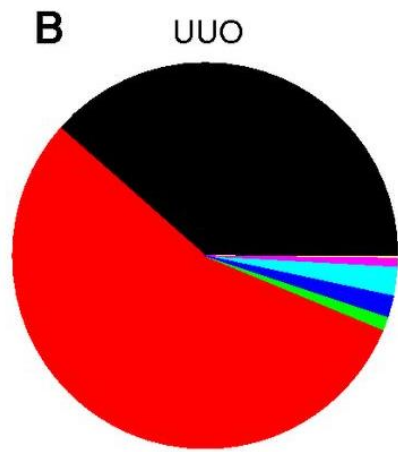
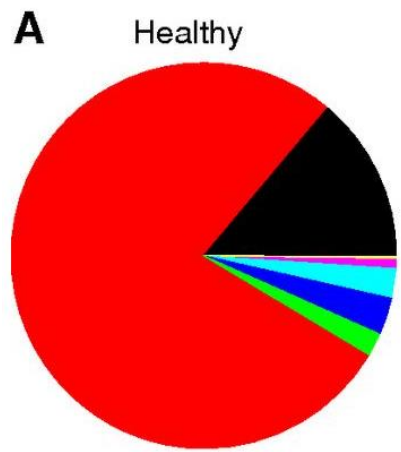


RESULTS

- Overall segmentation accuracy measured by Instance Dice Scores:
91.9% **Tubule**, 94.7% **Tuft**,
96.5% **Glom.**, 84.1% **Artery**,
78.2% **Lumen**, 94.2% **Vein**
- High generalization performance on an external test set and a held-out murine disease model
- Strong correlation with current “gold” standard methods (e.g. quantitative immunohistochemistry)

CONCLUSION

Accurate multispecies-, multimodel deep learning WSS enables automated quantitative analysis of renal histopathology and facilitates high-throughput experimental nephropathology



Mouse Models

UUO = unilateral ureteral obstruction
 IRI = ischemia-reperfusion injury
 Adenine-induced nephropathy
 Alport: Col4a3 knock-out
 NTN = nephrotoxic serum nephritis

Relative area distributions of automatically segmented classes. The relative area distributions in percentages in (A) healthy, (B) UUO, (C) IRI, (D) adenine, (E) Alport, and (F) NTN kidneys additionally give information on the proportion of remaining nonclassified tubulointerstitial area (shown in black).

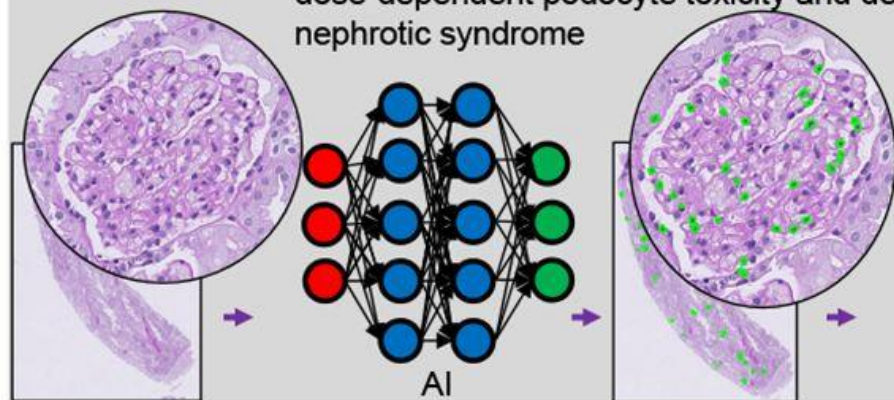
PodoSighter: A Cloud-Based Tool for Label-Free Podocyte Detection in Kidney Whole Slide Images

JASN

JOURNAL OF THE AMERICAN SOCIETY OF NEPHROLOGY

Methods

- 122 histologic sections, 3 species (mouse, rat, and human)
- Diseases - diabetic kidney disease, crescentic glomerulonephritis, dose-dependent podocyte toxicity and depletion, steroid-resistant nephrotic syndrome

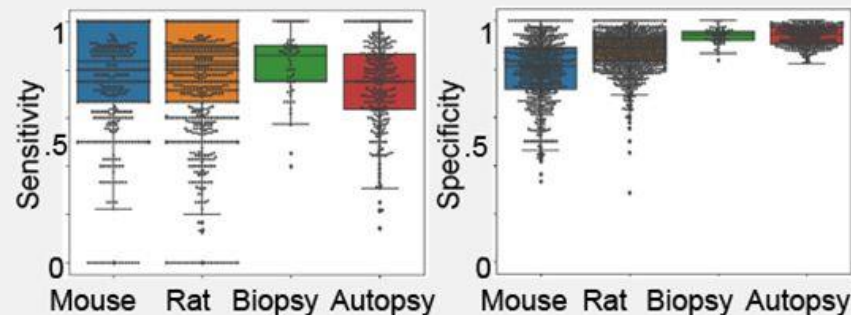


- Average podocyte counts per glomerulus
- Podocyte volume density per whole slide image (WSI)

Quantification

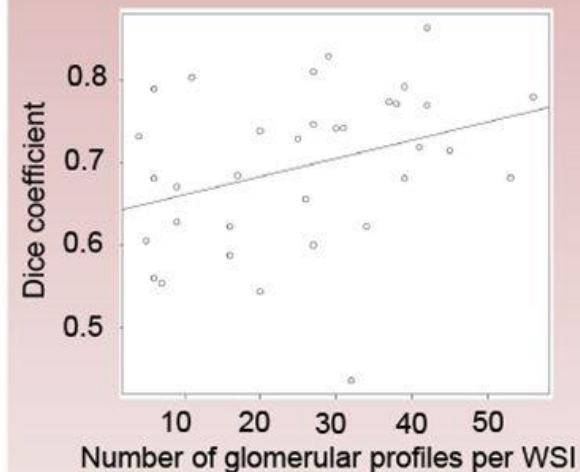
Results

- **Network sensitivity/specificity:**
Mouse - 0.80/0.80,
Rat - 0.81/0.86,
Human - 0.80/0.91
- Low absolute error
(0.47 ± 0.49 podocytes per $10^4 \mu\text{m}^3$) compared to ground-truth podocyte volume density



Conclusions

- Deep learning networks demonstrate high performance in detecting podocyte nuclei regardless of species and disease state.
- Networks detect podocyte density loss in diseased cases compared to control.
- Performance increases with increase in number of glomerular profiles per WSI.



Sarder Lab Slide Analyzer darshanagovind / Public / JPH12.svs Annotated images... Open image... Analyses darshanagovind

IO

Data folder
Select the folder containing all files
Choose a folder...

Input PAS whole slide image
Input PAS-stained svcs whole slide image
JPH12.svs

Input Glomerular Annotation File
Input glomerular annotation file (*.xml)
Choose a file...

Train Generator Model
Trained Generator Model (*.pth)
Choose a file...

Trained Discriminator Model
Trained Discriminator Model (*.pth)
Choose a file...

JSON format podocyte nuclei annotation filename
Output annotation file (*.anot) containing annotations
PodoSighter_pix2pix-outputAn



GlomArea V1

PodoSighter_CNN
PodoSighter_pix2pix
PodocyteDetection
TranslateXMLToJson
glom_getcsv

dsarchive/histomicstk
sarderlab/histo-cloud
sarderlab/podosighter

Zoom
25.1
Fit 2.5 5 10 20 40 80
Download View Download Area

Metadata
Annotations
Other
☐ Labels ☐ Interactive New

PodoSighter plugin on the cloud. The layout of the PodoSighter pipeline is shown here, along with a representative PAS image from a human renal biopsy. The podocyte nuclei predicted by one of the networks are highlighted in green.

Podocytes and Proteinuria in ANCA-Associated Glomerulonephritis: A Case-Control Study

Emma E. van Daalen^{1*}, Peter Neeskens¹, Malu Zandbergen¹, Lorraine Harper², Alexandre Karras³, Augusto Vaglio⁴, Janak de Zoysa⁵, Jan A. Bruijn¹ and Ingeborg M. Bajema¹

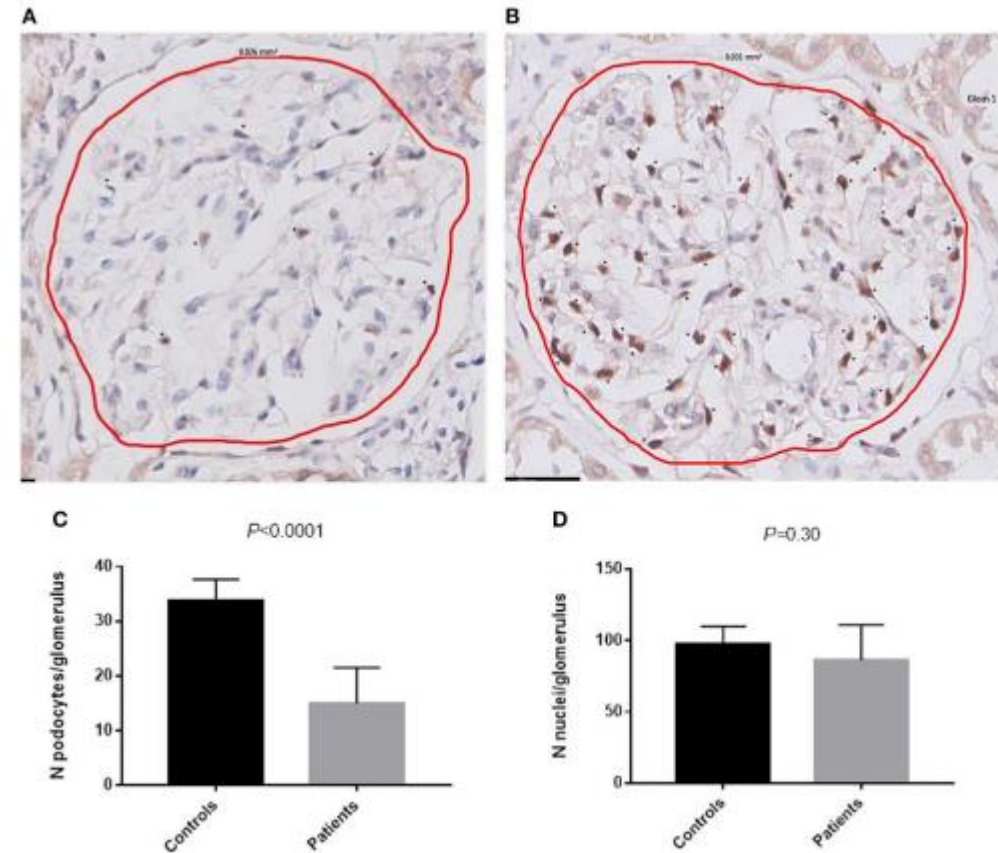
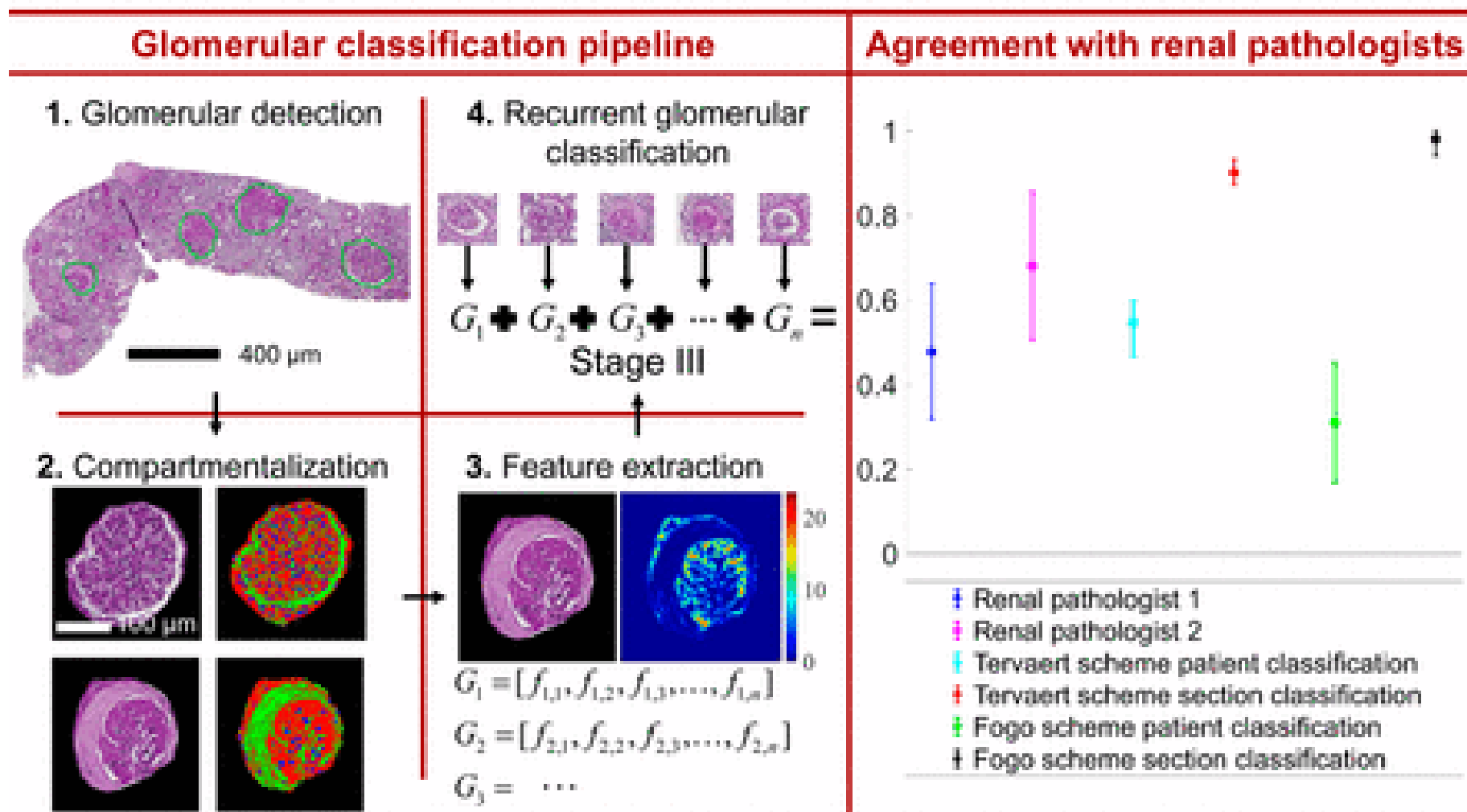


FIGURE 3 | Podocytes positive for WT-1. **(A)** WT-1 staining in a glomerulus of a patient with AAGN. **(B)** WT-1 staining in a glomerulus of a control. Asterisks (*) indicate a podocyte positive for WT-1. **(C)** Number of podocytes per glomerulus in controls and in patients ($P < 0.0001$). **(D)** Number of nuclei per glomerulus in controls and in patients.

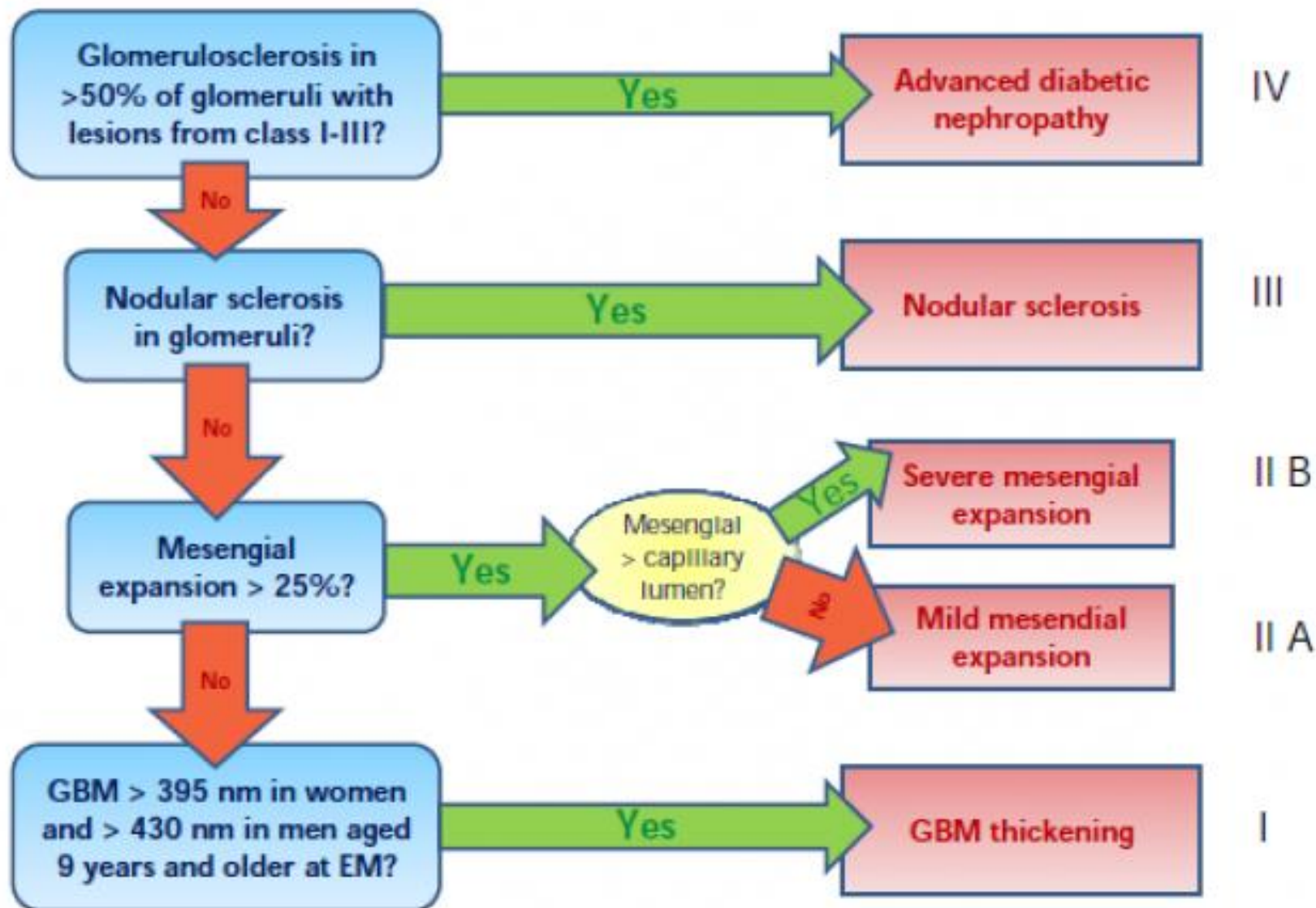
Computational Segmentation and Classification of Diabetic Glomerulosclerosis



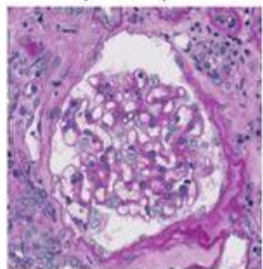
CONCLUSION

Digital, quantitative, structural analysis can enhance diagnostic objectivity.

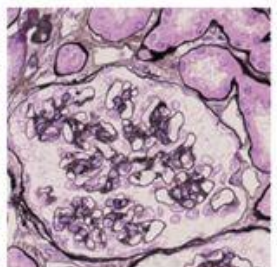
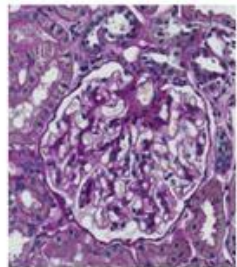
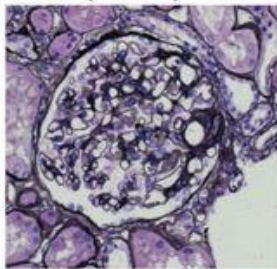
doi: 10.1681/ASN.2018121259



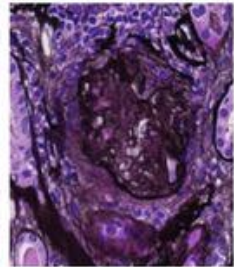
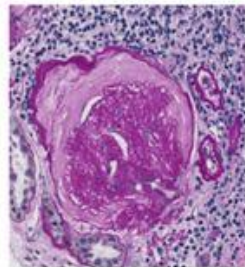
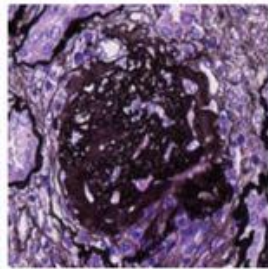
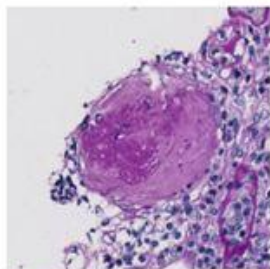
Normal Glomerulus
(PAS)



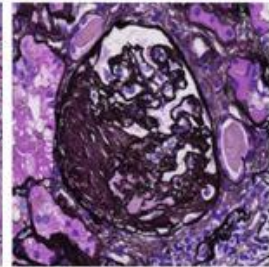
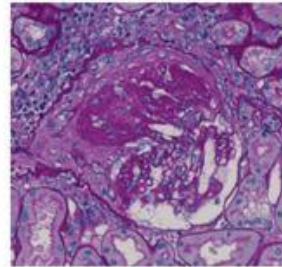
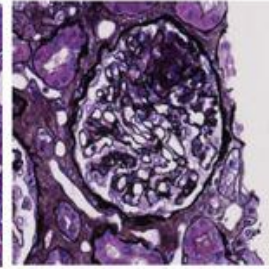
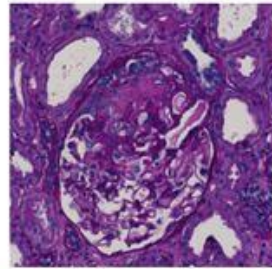
(PAM)



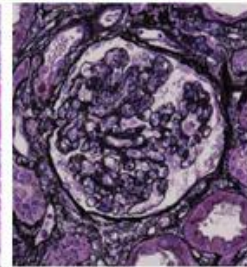
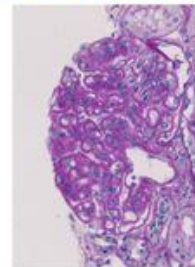
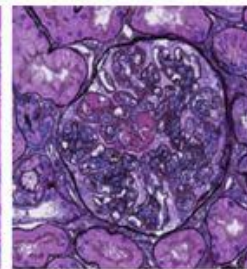
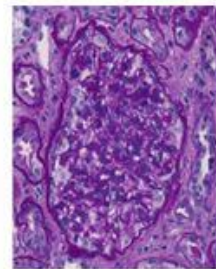
Global Sclerosis



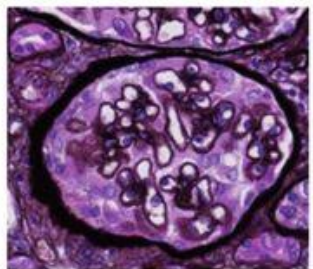
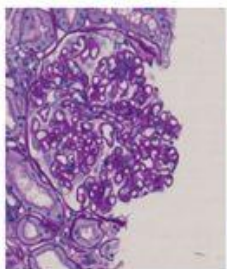
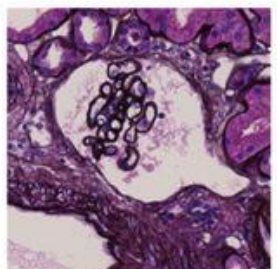
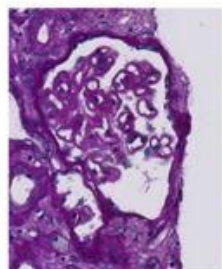
Segmental Sclerosis



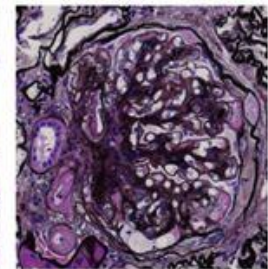
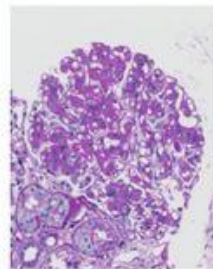
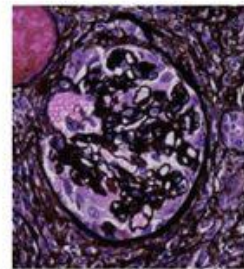
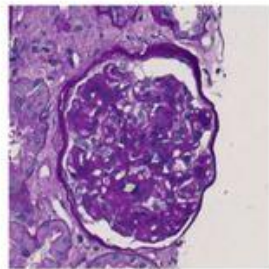
Endocapillary
Proliferation



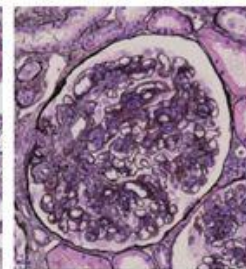
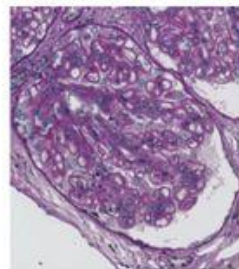
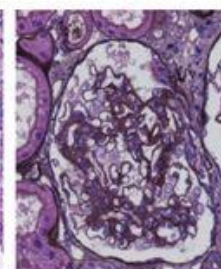
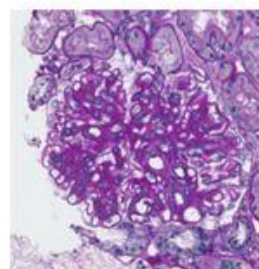
Basement Membrane
Structural Changes



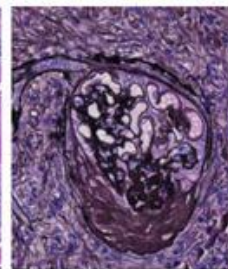
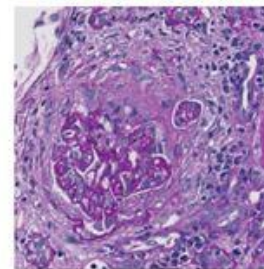
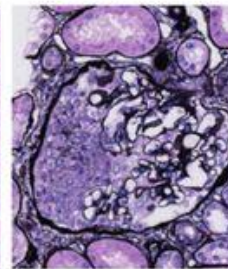
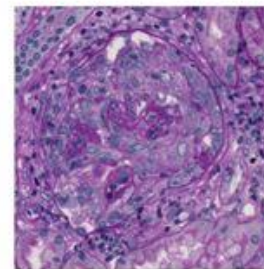
Mesangial Matrix
Accumulation



Mesangial Cell
Proliferation



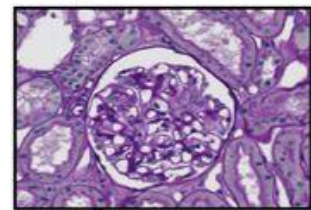
Crescent



Classification of glomerular pathological findings using deep learning and nephrologist-AI collective intelligence approach

① Eiichiro Uchino, Kanata Suzuki, Noriaki Sato, Ryosuke Kojima, Yoshinori Tamada, Shusuke Hiragi, Hideki Yokoi, Nobuhiro Yugami, Sachiko Minamiguchi, Hironori Haga, ① Motoko Yanagita, Yasushi Okuno

Input: Glomerular image



fine-tuned CNN
(InceptionV3)

Classification

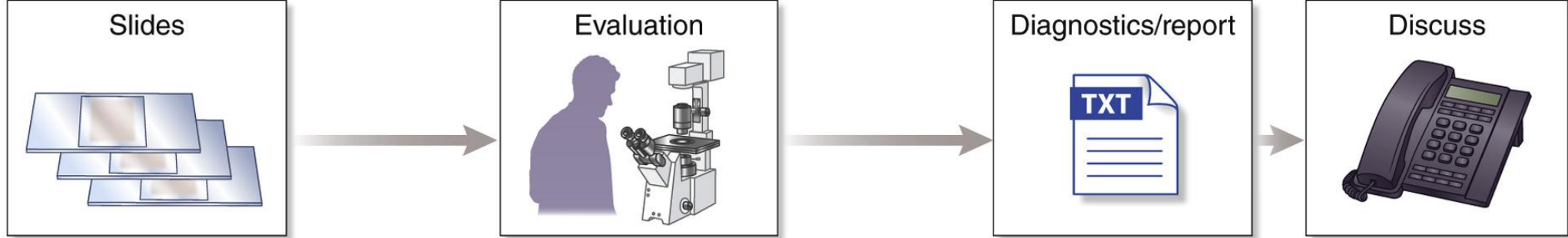
Positive

Negative

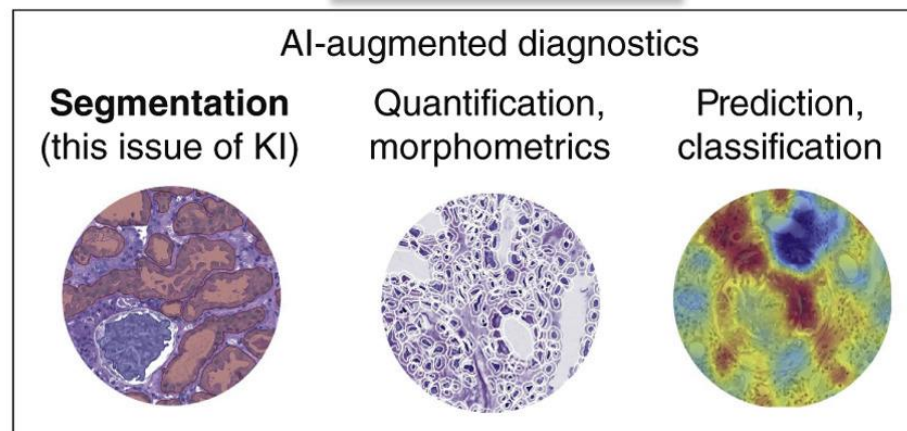
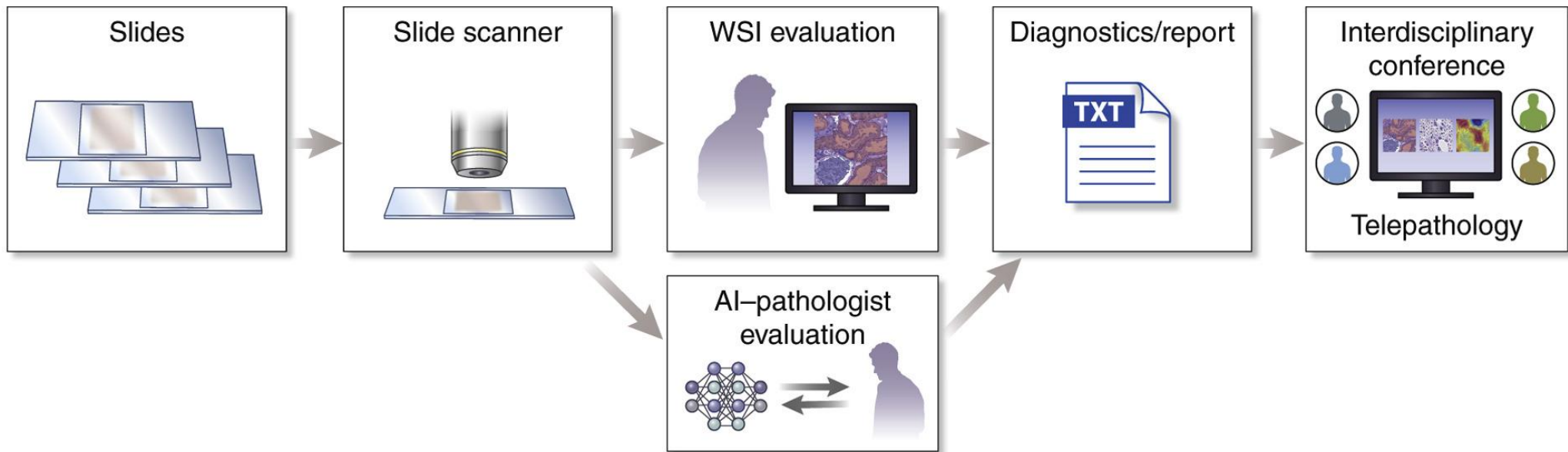
(for each finding)

- Convolution
- AvgPool
- MaxPool
- Concat
- Dropout
- Fully connected
- Softmax

Analog workflow



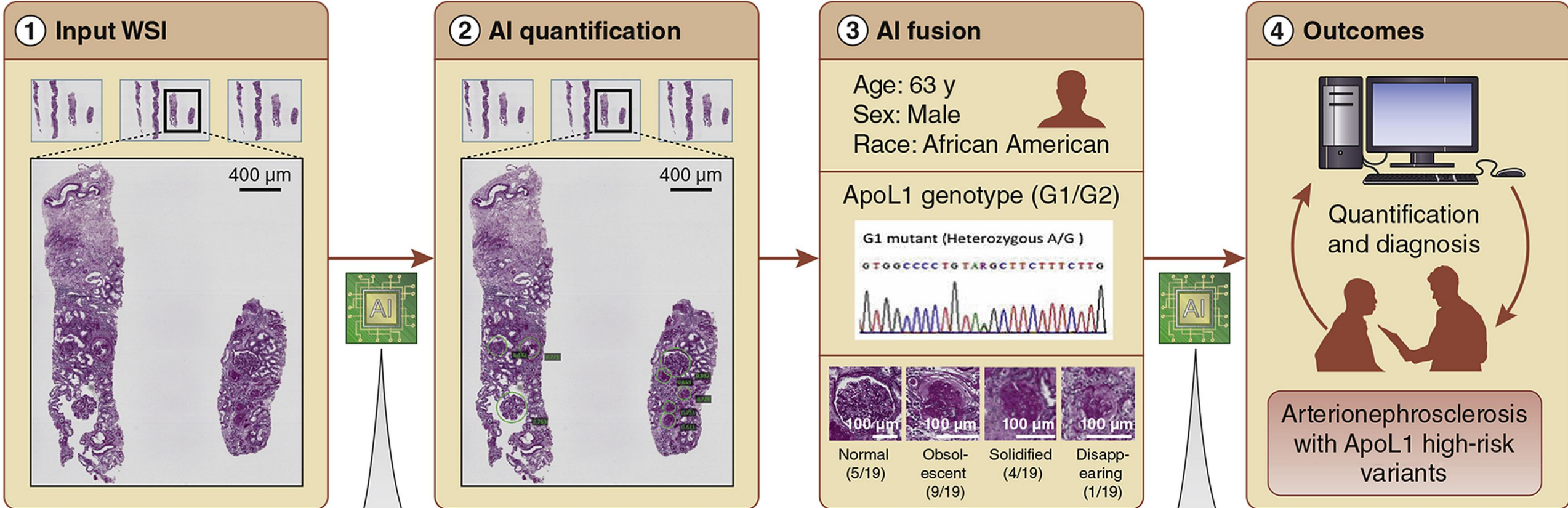
Digital workflow



COMMENTARY | VOLUME 99, ISSUE 1, P17-19, JANUARY 01, 2021

Multistain segmentation of renal histology: first steps toward artificial intelligence-augmented digital nephropathology

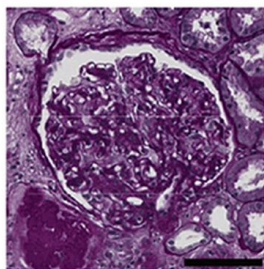
Roman D. Bülow • Jesper Kers • Peter Boor



Standard task in AI quantification

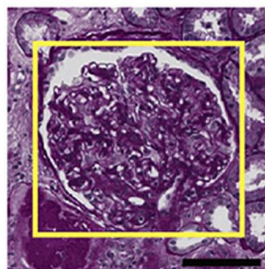
Image-level

Classification



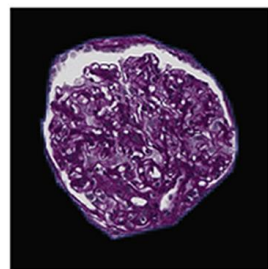
Region-level

Detection



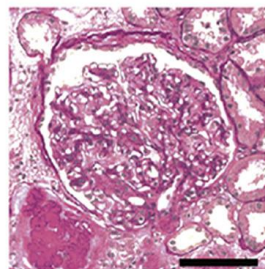
Pixel-level

Segmentation



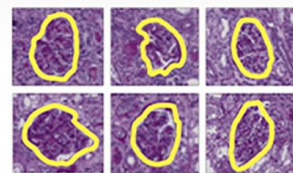
Domain-level

Synthesis



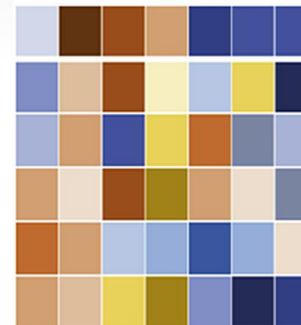
Typical modalities for AI fusion

Image features



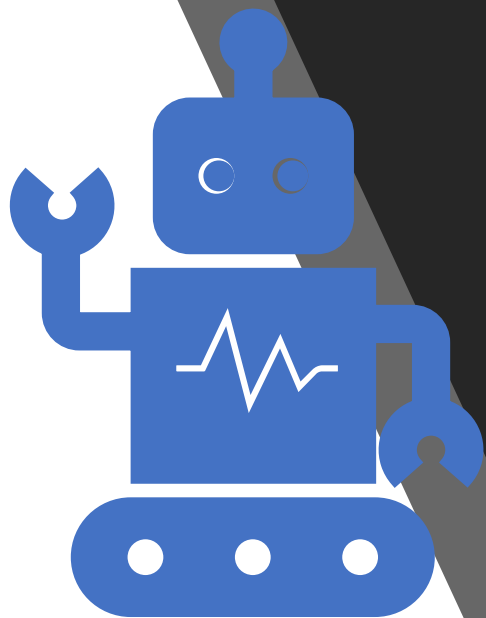
S#	G#	Image	Diagnose
1	001		Normal
1	002		GDG
1	003		GOG

Omics features



Clinical features

	A	B	C	D
1	PatientID	Age	Sex	Race
2	p-0001	49	male	C
3	p-0002	48	female	B
4	p-0003	25	male	A
5	p-0004	71	male	L
6	p-0005	32	female	H
7	p-0006	56	female	N
8	p-0007	62	male	C
9	p-0008	32	male	B
10	p-0009	67	female	A
11	p-0010	71	male	C
12	p-0002	21	female	C
13	p-0003	32	female	C



Points for discussion

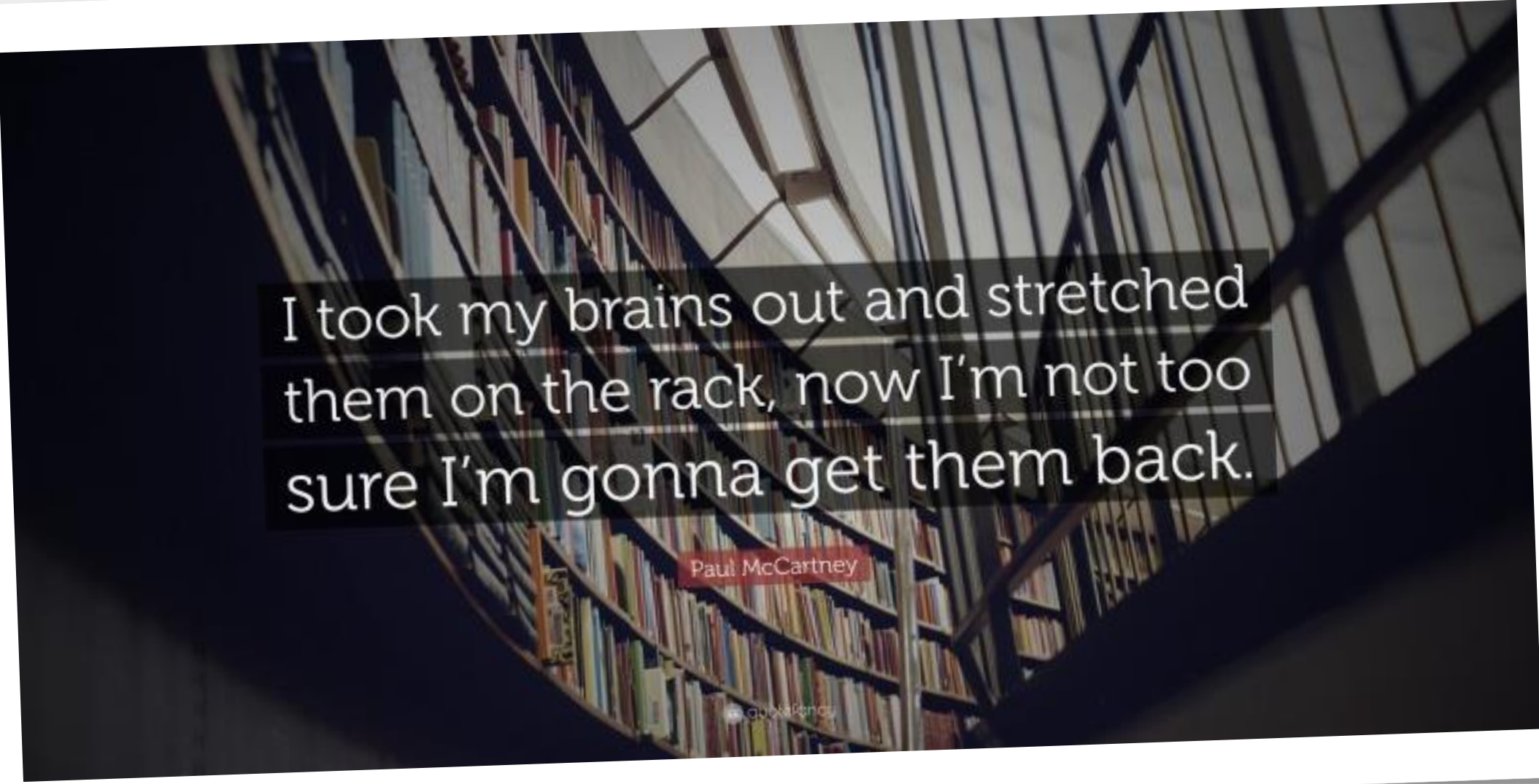
What do you expect from AI in relation to histopathology in the near future?

What are benefits, how can we work on getting it right?

What about interobserver variability?

How will we learn from AI in medicine – or will we ‘unlearn’?

Matters not yet discussed...



I took my brains out and stretched
them on the rack, now I'm not too
sure I'm gonna get them back.

Paul McCartney

quaxagency